P9.4 WRF-enabled diagnosis of the 12 March 2006 severe weather outbreak

Anthony Reinhart *[1] and Robert J. Trapp[2]
[1]University of Nebraska, Lincoln, NE
[2]Purdue University, West Lafayette, IN

1. Introduction

The severe weather outbreak on 12 March 2006 involved several long-lived long track tornadic supercells. One such supercell spawned 22 tornadoes and produced damaging hail throughout Missouri, Illinois, and parts of Kansas. This storm had an 885-km track that began in eastern Oklahoma, and possessed supercellular characteristics during its thirteen-hour life.
Given the typical supercell lifetime of a couple hours (e.g., Bunkers et al. 2006a), we consider this an exceptionally long-lived storm.

Herein we use the conventional meteorological data stream in concert with a real-data numerical simulation to study the initiation, propagation, and demise of the long-lived supercell thunderstorm that occurred on 12 March 2006.

2. Observations

2.1 Overview of Synoptic Conditions

A surface low was positioned in southeastern Colorado at 12 UTC on 12 March. A surface warm front extended from eastern Colorado through northern Oklahoma. A stationary front was present over Missouri and a cold front stretched through Illinois and Indiana. A dry line was located through central Oklahoma and central Texas.

As the day progressed, the surface low moved northward into extreme western Kansas. The 1800 UTC surface analysis showed the warm front located through northern Kansas, Missouri, Illinois, and Indiana. Satellite data at this time indicated that the dryline was located in eastern Kansas, Oklahoma, and Texas. A bulge in the dryline was also present, as seen in satellite water vapor images. The dryline bulge stemmed from stronger and more of a westerly component than the surface winds (Schaefer, 1986; Peckham et al., 2004; Auslander and Bannon, 2004; Limpert et al. 2006). This localized rapid propagation of the dryline and increased convergence along it allowed for enough forcing to break the capping inversion.

Strong upper-level forcing was present in the form of a 115 kt, 300 hPa (70 kt, 500 hPa) jet positioned over the Great Plains, with a deep trough 500 hPa located over the Intermountain West. The strong winds aloft also allowed deep vertical wind shear supportive of supercell development.

2.2 Convective Initiation

In apparent association with the dryline bulge, radar images at ~1800 UTC showed the initiation of cells in far northeastern Oklahoma and far southeastern Kansas. Per a special 1800 UTC sounding launched from Springfield, Missouri, these cells initiated in a favorable environment characterized by CAPE of 1650 J kg^{-1} and 0 to 6 km shear of 45 kts.

2.3 Supercell Propagation and Lifecycle

In order to examine the evolution of the long-lived supercell, WSR-88D radar data were gathered from sites nearest to the supercell (KICT, KEAX, KLSX, KILX, and KLOT). Cells and mesocyclones were identified and tracked using the netssap algorithm in WDSS (Lakshmanan et al. 2007). The presence of a MDA was used to determine if a cell was a supercell.

About thirty minutes after initiation, as the thunderstorms moved into Missouri, they began to exhibit supercellular characteristics. Cell splitting occurred at 1838 UTC, and this was when the storms began to track to the right of the mean wind. Around this same time the MDA began to detect mesocyclones in the newly formed supercells.

The 2000 UTC RUC analysis showed the warm front extending across central Missouri, and further showed that north of the warm front there was little CAPE. One of the three supercells

* *Corresponding author address:* Anthony E. Reinhart, Department of Geosciences, University of Nebraska – Lincoln, 214 Bessey Hall, Lincoln, NE 68588. Email: aereinha@huskers.unl.edu

moved across the boundary and lost supercellular characteristics. The other two supercells remained close to the warm front in an area of enhanced shear and CAPE.

The first tornado occurred around 2150 UTC near Calhoun, Missouri. The supercell remained tornadic from 2150 UTC through 2230 UTC. As the supercell tracked northeastward a second round of tornadoes were spawned over eastern Missouri between 2330 UTC and 0030 UTC. As the supercell crossed the Mississippi River, the northern of the two cells crossed the warm front and began to transform into a multicell line.. The southern cell experienced rapid intensification as it moved over western Illinois. The supercell produced several tornadoes in downtown Springfield, Illinois, and others during the next two hours.

The long-lived supercell began its transition period when it crossed into Indiana. The supercell became less isolated as a developing QLCS approached from the west. The supercell lost its rotation characteristics just before merging with the QLCS around 0700 UTC.

4. Model Simulation

The Advanced Research core of the Weather Research and Forecasting model (WRF) version 2.1 was used for the real data numerical simulation (Skamarock et al. 2005). The initial condition data came from the North American Regional Reanalysis (NARR) dataset. Horizontal gridpoint spacing was 12 km for the outer domain, which covered most of the central United States. A 4 km two-way nested domain was centered over Missouri and Illinois (figure 1).

The model simulation began at 00 UTC on 12 March 2006, approximately 18 h before convective initiation, and ran through 1200 UTC on 13 March 2006. Kain-Fritsch convective parameterization scheme was used for the outer domain, and no convective parameterization was used on the nested domain, which is considered fine enough to resolve the evolution and key structural features of convective systems (Kain et al. 1993 and Weisman et al. 1997). A 4-km gridpoint spacing in WRF has also been shown to provide enough detail to detect mesocyclones (Kain et al. 2008).

4.1 Simulation of Synoptic-Scale Conditions

A properly situated warm front and dryline were shown in the simulation fields. Otherwise, the simulated synoptic-scale system evolved similar to the observed system, with the exception of a southward displacement in system movement. This ultimately led to the southward displacement of convective storms by about 35 km.

4.2 Supercell initiation and evolution

Although convective initiation occurred nearly two hours late, the simulated cells were nearly geographically collocated with the actual cells at 20 UTC (figure 2). These several cells then coalesced into three main cells exhibiting supercellular characteristics. The southernmost located cell became the long-lived supercell.

The supercell propagation throughout the simulation was very similar to the real data observations. The main difference was the initiation period, and the slight displacement of the long-lived supercell. The displacement is attributed to the differences between synoptic conditions of the simulation and the real data observations.

4.3. Model Detected Supercelluar Characteristics and Tornadoes

Supercells occurring in this numerical simulation were determined through several means of varying importance. Simulated reflectivity plots allowed for qualitative assessment of storm structure. The model data also allowed for the calculation of vertical velocity and vertical vorticity for quantitative identification of supercells (Davies-Jones 1984; Droegemeier et al. 1993; Wicker et al 2005). Here, we used a form of the Supercell Detection Index (SDI), which was used in recent forecast experiments at the SPC and NSSL (Weiss et al. 2007). For this study, a parameter *S* was defined at each gridpoint within the nested domain as

$$S = \left\langle \frac{w\zeta}{\left(w^2\zeta^2\right)^{1/2}} \right\rangle,$$

where *w* is the vertical velocity, ζ is vertical vorticity, and the brackets mean a vertical average of each grid column from the surface to 5 km (Trapp et al. 2006). Not all supercells or mesocyclonic storms create tornadoes (e.g., Trapp et a al. 2005).

SDI and S values of 0.6 have been used in the past as the demarcation between nonsupercellular and supercellular storm with possible tornado (Trapp et al. 2006; Weiss et al. 2007). This study also suggests that a value greater than 0.9 could be used as the demarcation between supercell and supercell with a high likelihood of a tornado.

Using this parameter as a guide, we found that the WRF model produced a long-lived supercell that matched spatially the observed long-lived supercell. A temporal matching was also found: At every timestep the model output detected a supercell that corresponded to an actual supercell (Figure 3).

The WRF simulation suggests a relationship between the *S* parameter and tornado occurrences. This is in part based on tornado tracks from detailed in the NCDC storm report database. The tornado occurrences were during three distinct temporal intervals: between 2150 - 2233 UTC, 0000 - 0045 UTC, and 0130 – 0400 UTC. The *S* associated with the simulated supercell was ≥ 0.9 from 2200 - 0330 UTC, and from 0400 - 0530 UTC. However, this does not take into account the time bias due to the delayed convection initiation. Upon using spatial comparisons as well, a contingency table (Table 1) shows that the WRF model does well at simulating a potentially tornado supercell when a tornado was occurring. In particular, the Heidke skill score shows a 0.9 relationship between the *S* parameter and tornadoes.

5. Discussion and Summary

The longevity of the 12 March 2006 supercell was due to the synoptic conditions that favored storm propagation relative to the northeast lifting the warm front. This allowed the supercell to remain in the very favorable environment for the duration of its life. Furthermore, an inversion in the environment south of the supercell track allowed the supercell to remain isolated.

The WRF simulation provides further evidence that model fields can be used to quantitatively identify supercell mesocyclones (Kain et al. 2008). A parameter based on gridpoint values of vertical velocity and vertical vorticity suggests that it is also possible to assess the probability of a supercell to be tornadic.

6. Figures and Table

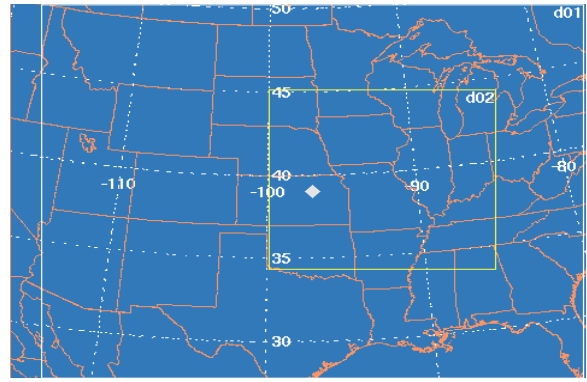

Figure 1: WRF simulation domain size and location

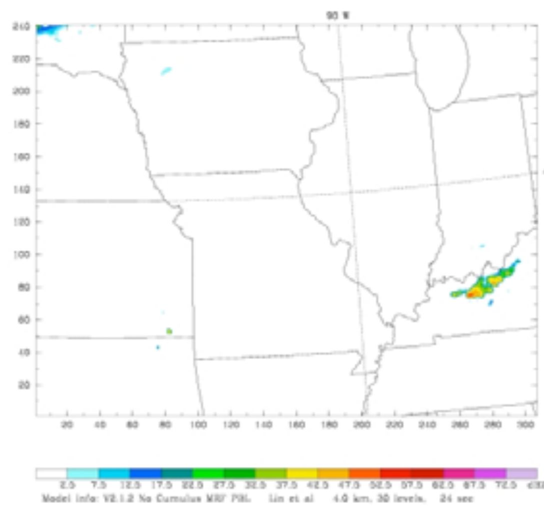

Figure 2: Model Reflectivity at the time of Convective Initiation

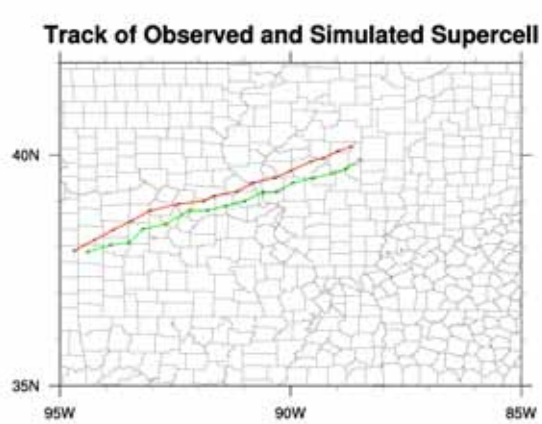

Figure 3: Observed and simulated supercell tracks over time. The red line is the path of the observed supercell. Green is the path of the simulated supercell. The average distance between the two is 37 km.

	Model indicated tornado	
Observed Tornado	Yes	No
Yes	10	0
No	2	2

Table 1: Contingency table containing the number of numerical model indicated possible tornadoes and observed tornadoes.

7. References

Auslander, G.M. and P. R. Bannon, 2004: Dryline bulge evolution in a two-dimensional mixed-layer model. *J. Atmos. Sci.*, **61**, 2528-2543.

Bunkers, M.J., M.R. Hjelmfelt, and P.L. Smith, 2006: An Observational examination of long-lived supercells. Part I: characteristics, evolution, and demise, *Wea. and Forecasting,* **21,** 673 - 688

Bunkers, M.J., J.S. Johnson, L.J. Czepyha, J.M. Grzywacz, B.A. Klimowski, and M.R. Hjelmfelt 2006b: An observational examination of long-lived supercells. Part II: environmental conditions and forecasting, *Wea. and Forecasting*, **21**, 689 – 714.

Davies-Jones, R. P., 1984: Streamwise vorticity: The origin of updraft rotation in supercell storms, *J. Atmos. Sci.,* **41**, 2991-3006.

Droegemeier, K. K., S. M. Lazarus, and R. P. Davies-Jones, 1993: The influence of helicity in numerically simulated convective storms, *Mon. Wea. Rev.,* **121**, 2005-2029.

Kain, J. S., and J. M. Fritsch, 1993: Convective parameterization for mesoscale models: The Kain-Fritcsh scheme, The representation of cumulus convection in numerical models, K. A. Emanuel and D.J. Raymond, Eds., Amer. Meteor. Soc., 246 pp.

Kain, J.S., S.J. Weiss, J.J. Levit, M.E. Baldwin, and D.R. Bright, 2008: Some practical considerations regarding horizontal resolution in the first generation of operational convection-allowing NWP, *Wea. Forecasting,* in press.

Lakshmanan, V., T. Smith, G. J. Stumpf, and K. Hondl, 2007: The warning decision support system - integrated information (WDSS-II). Weather and Forecasting, 22, No. 3, 592-608

Limpert, G. L., E. Sutton, C. Heck, N. Fox,C. Schultz, 2006: A case study of a long-lived supercell in the 12 March 2006 severe weather outbreak. Prepreints, 23rd Conf. on Severe Local Storms, St. Louis, Mo.

Peckham, S.E., et al., 2004: Numerical Simulation of the interaction between the dryline and horizontal convective rolls. *Mon. Wea. Rev.,* **132**, 1792-1812.

Schaefer, J.T., 1986: The dryline. Mesoscale Meteorology and Forecasting, P. S. Ray, Ed., Amer. Meteor. Soc., 549-572.

Skamarock, W.C., J.B. Klemp, J. Dudhia, D.O. Gill, D.M. Barker, W. Wang and J.G. Powers, 2005: A description of the Advanced Research WRF Version 2, NCAR Tech Note, NCAR/TN-468+STR, 88 pp.

Trapp, R. J., B. A. Halvorson, and N. S. Diffenbaugh, 2006: Telescoping model approaches to evaluate severe convective storms under future climates. Preprints, 23rd Conf. on Severe Local Storms, St. Louis, Mo.

Trapp, R. J., G. J. Stumpf, and K. L. Manross, 2005: A reassessment of the percentage of tornadic mesocyclones. *Wea. Forecasting*, **20**m 680-687.

Weisman, M.L, W.C. Skamarock, and J.B. Klemp, 1997: The resolution dependence of explicitly modeled convective systems, *Mon. Wea. Rev.*, **125**. 527- 548

Weiss, S., J. Kain, D. Bright, J. Levit, G. Carbin, and M. Coniglio, 2007: SPC/NSSL Spring program 2005: Program overview and operations plan.